Korea-Australia Rheology Journal, Vol.24, No.3, pp.147-153 (2012) www.springer.com/13367
DOI: 10.1007/s13367-012-0018-x

Review

Field-responsive smart composite particle suspension: materials and rheology

Wen Ling Zhang, Ying Dan Liu and Hyoung Jin Choi*
Department of Polymer Science and Engineering, Inha University, Incheon, 402-751, Republic of Korea
(Revised August 20, 2012; final revision received August 27, 2012; accepted August 30, 2012)

Abstract

Both electrorheological (ER) and magnetorheological (MR) fluids are known to be smart materials which can be rapidly and reversibly transformed from a fluid-like to a solid-like state within milliseconds by showing dramatic and tunable changes in their rheological properties under external electrical or magnetic field strength, respectively. Here, among various smart composite particles studied, recently developed core-shell structured polystyrene/graphene oxide composite based ER material as well as the dual-step functionally coated carbonyl iron composite based MR material are briefly reviewed along with their rheological characteristics under external fields.

***Keywords*:** rheology, electrorheological fluid, magnetorheological fluid, microsphere, graphene oxide

1. Introduction

Electro-responsive electrorheological (ER) fluids are composed of polarizable particles dispersed in insulating oils such as mineral, paraffin or silicone oils (Kim and Jung, 2010; Orihara *et al*., 2011; Yin *et al*., 2011), likewise, the analogous magnetorheological (MR) suspensions composed of soft magnetic particles suspended in nonmagnetic medium (Bica, 2011; Hiamtup *et al*., 2010; Huo *et al*., 2011; Li and Zhang, 2008; Wang, *et al*., 2009). These smart ER and MR materials can be rapidly and reversibly transformed from a liquid-like to a solid-like state within milliseconds by controlling external electrical or magnetic field strength, respectively. Thereby these materials show dramatic and tunable changes in their rheological properties such as yield stress, apparent shear viscosity and storage modulus. They thus have attracted considerable attention for various engineering applications such as dampers, torque transducers, or polishing devices (Choi and Jhon, 2009; Niu *et al*., 2009). ER smart/intelligent materials include various electro-responsive materials like conducting polymers, inorganic materials such as silica and clay, mesoporous materials and polymer composites, while magnetic particles for the MR fluids are soft magnetic materials with less magnetic hysteresis such as carbonyl iron (CI) and iron alloys. Among various ER smart materials, core/shell structured composites including poly(methyl methacrylate)/polyaniline (PANI) composite, PANI coated snowman-like particle, and the MR fluids with CI core/polymers or carbon nanotubes (CNT) shell have been reported (Fang *et al*., 2010a; Lee *et al*., 2005; Liu *et al*., 2010; Sedlacik *et al*., 2010; Tang *et al*., 2000).

As an ER smart material, the electrical conductivity value is a critical parameter which has to be met in the semi-conducting regime of about 10^{-6}~10^{-10} Scm^{-1} to avoid an electric short circuit of the rheometer during the test, thereby the composites which were made up of semiconducting polymers or polarizable inorganics are considered as good ER material candidates (Tian *et al*., 2001; Cho *et al*., 2003, Yin *et al*., 2009). Recently, we reported the typical ER characteristics of graphene oxide (GO)/PANI nanocomposite based ER fluid under an applied electric field (Zhang *et al*., 2010). Here, graphene, the recently introduced material with a sp^2-bonded carbon honeycomb lattice which is the mother building unit of its other well-known allotropes such as fullerene, carbon nanotubes and graphite, has attracted tremendous attention due to its extraordinary electrical, thermal, mechanical, and structural properties (Fang *et al*., 2010b). As an excellent choice for fabricating various unique and multifunctional composites, graphene-based materials have potential applications in a variety of industries including chemical sensors, field-effect transistors, transparent conducting films, sensors, supercapacitors, nanoelectronics, batteries, and so on (Barnard and Snook, 2010; Cai and Song, 2010; Kampouris and Banks, 2010; Wu *et al*., 2010). However, the large and facile mass production of graphene with a reasonable price is still a hot topic for many scientists. Up to now, the exfoliation of graphite oxide which can be produced by oxidation of graphite in the presence of strong acids and oxidants is one of the most effective ways to prepare the GO. Compared to the graphene, the GO possesses a wide

This paper is based on an invited lecture presented by the corresponding author at the 12th International Symposium on Applied Rheology (ISAR), held May 17, 2012, Seoul.
*Corresponding author: hjchoi@inha.ac.kr

range of interesting characteristics due to these functional groups, typically its good dispersion stability in aquous and other common organic slovents (Stankovich *et al*., 2007) which facilates the preparation of polymer-GO composites. Even rather a poor electrical conductivity (10^{-6} S cm^{-1}) of the GO is conversely appropriate in the ER study. Thereby, the GO based ER fluid has been recently reported (Hong and Jang, 2012; Zhang *et al*., 2012b). Among various GO based composite materials developed recently, the core/shell structured polystyrene (PS)/GO composite can provide suitable conductivity as an ER material via adjusting appropriate proportion of PS and GO.

Likewise, the MR fluids act as free-flowing liquids without an external magnetic field but reversibly transform to a plastic-like solid within milliseconds with an external magnetic field applied. Carbonyl iron particles are considered as superior MR candidates with various outstanding merits such as a proper particle size, activity over a broad temperature range and high yield stress under an applied magnetic field (Jang *et al*., 2005; Tian *et al*., 2010). However, severe sedimentation and agglomeration problems of the dispersed particles while preparing and measuring the MR fluids due to the large density mismatch and the physical contact of CI particles need to be improved. Various ways to overcome these issues such as introducing additives of gap-filler and polymer coating have been introduced (Lim *et al*., 2005; Ngatu and Wereley, 2007; Zhang *et al*., 2008). The polymer coating technique appears to be one of the best options for stabilizing MR fluid suspensions with the decreased density of CI/polymer composite particles compared to that of the pristine CI particles.

Here, as an MR system, we review a recently reported two-step coating process to introduce polystyrene shell and a MWNT nest on the CI particle surfaces to improve the sedimentation problems associated with CI based MR suspensions (Fang *et al*., 2010a).

2. Field-responsive Smart Composite Particles

2.1. GO/PS core-shell electro-responsive composite

The GO is generally prepared by the exfoliation of graphite oxide according to the modified Hummers method (Hummers and Offeman, 1958). The core–shell structured PS/GO composite can be formed due to the strong π–π stacking interaction between PS microspheres and GO sheets (Zhang *et al*., 2011), in which monodispersed PS microspheres were prepared using a dispersion polymerization.

Fig. 1 shows the SEM images of PS/GO composite particles, the surface of the core/shell structured PS/GO composite particles became much rougher due to the creamy GO sheets wrapping over the particles. In addition, the GO sheet is nearly uniformly spread over the surface of PS microsphere, demonstrating that the sonication provides well dispersion of the GO sheets.

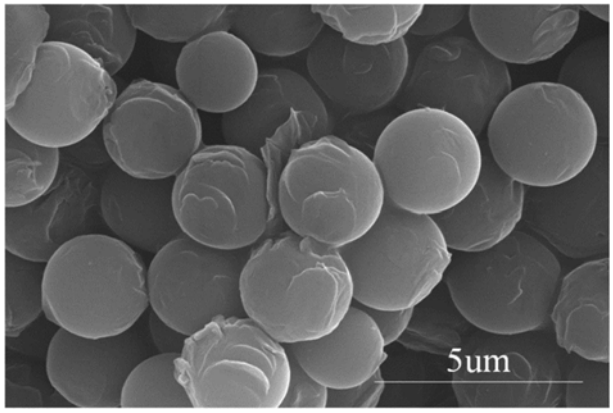

Fig. 1. SEM image of PS/GO nanocomposite (Reprinted from Zhang *et al*., 2011).

2.2. GO/PANI electro-responsive composite

The GO/PANI composite particle was fabricated via in situ oxidation polymerization in the presence of GO prepared via a modified Hummers method without a dopant, in which the GO was individually exfoliated. The low electrical conductivity and acidic groups of GO, which are disadvantages in many investigations, become positive and favorite factors in the ER study. A low conductivity can reduce the possibility of short-circuits and acid groups can be used as dopant sites of PANI. Zhang *et al*. (2010) were the first to report ER response of the GO related material system.

2.3. MWNT/PS/CI magneto-responsive composite particles

The soft magnetic CI-based MR fluids could be improved by applying a dual-step functional coatings composed of polymeric polystyrene (PS) layer and a multi-walled carbon nanotube (MWNT) nest to the surfaces of the CI particles via a conventional dispersion polymerization and a facile water-in-oil emulsion process (Fang *et al*., 2010a).

The SEM images of CI particles before and after coating were shown in Fig. 2. The pristine CI particles had a very smooth surface with a polydispersed size distribution. After being coated by PS, many PS half-spheres with an almost monodispersed size distribution were spread over the surface of the CI particles which were treated by mathacrylic acid previously. indicating that the CI particles were covered with a thick shell. For the MWNT and PS dual-coated CI particles, many MWCNTs were piled together, forming a dense MWNT network over the entire surface of the PS/CI particles. Some considerable tiny PS beads were covered completely by the MWNT nests and were invisible. The surface of the MWNT/PS/CI particles was quite rough compared to that of the pure CI or PS/CI particles. By adopting this simple water-in-oil emulsion methodology, well dispersed MWNTs tended to aggregate

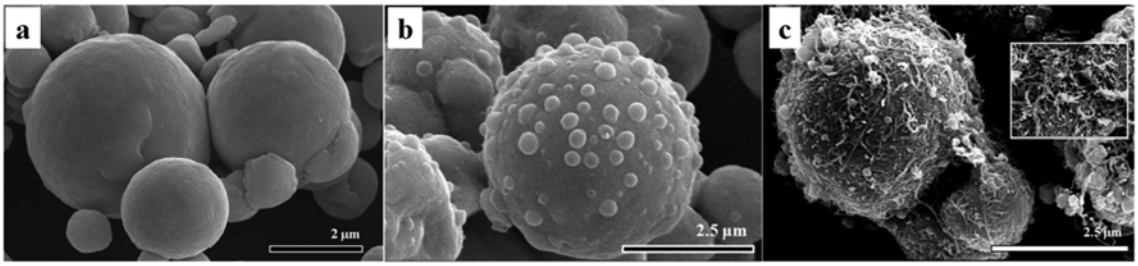

Fig. 2. SEM images of (a) pure CI (b) PS-coated CI and (c) MWNT wrapped PS/CI particles (the inset picture is SEM image of used MWNT) (Reprinted from Fang *et al*., 2010a).

by self-assembly around the surface of the PS/CI particles forming a dense nest when water was evaporated at high temperatures. The driving force was assumed to be nanotube-nanotube interactions and hydrogen bonding from the carboxyl groups and hydroxyl groups.

Furthermore, the soft magnetic CI-based MR fluids could be improved by applying a dual-step functional coatings composed of a conducting PANI layer and a multi-walled carbon nanotube nest to the surfaces of the CI particles via conventional dispersion polymerization and facile solvent casting (Fang *et al*., 2011).

3. Rheological Characteristics

The ER fluid was prepared by dispersing the products in silicone oil (0.955 g/cm^3, 30 cS), and the ER and MR properties were investigated by a rotational rheometer (Physica MCR300, Stuttgart, Germany) equipped with a high voltage generator using a Couette-type sample loading geometry with a bob and cup (CC 17, gap distance is 0.71 mm) and a MR device (MRD 180, Physica, Stuttgart, Germany) with a parallel plate geometry, respectively.

Furthermore, the shear stress as a function of shear rate for PS/GO composite particle based ER fluid was tested by a rotational rheometer equipped with a high voltage generator shown in Fig. 3. Without an electric field, the particle based ER fluid behaved similarly to a Newtonian-like fluid, in which the shear stress increases monotonically with the shear rate. When exposed to an external electric field, the dispersed particles got polarized and formed chain-like structure .

The typical Bingham fluid model (Cheng *et al*., 2009) as Eq. (1) has been widely adopted to express flow curves of many ER fluids :

$$\tau = \tau_0 + \eta_0\dot{\gamma}, \quad \tau \geq \tau_0$$

$$\dot{\gamma} = 0, \quad \tau < \tau_0 . \tag{1}$$

Here, τ_0 is the yield stress, which is related to an electric field, τ is the shear stress, $\dot{\gamma}$ is the shear rate, and η_0 is the shear viscosity. Many ER fluid curves cannot be fitted with this simple Bingham model over the whole shear rate region.

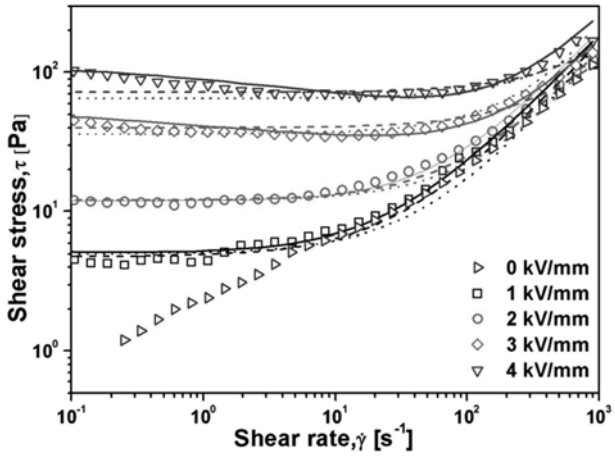

Fig. 3. Flow curves of 15 wt% core–shell structural PS/GO composite based ER fluid under different electric strengths. Solid, dash and dotted lines are from the CCJ model, De Kee–Turcotte model and Bingham model, respectively (Reprinted from Zhang, *et al*., 2011).

Thereby, other models named De Kee-Turcotte model (Kee and Turcotte 1980) and Cho-Choi-Jhon (CCJ) model (Cho *et al*., 2005) have been applied to fit these types of ER fluids well. The common form of De Kee-Turcotte model is $\tau = \tau_0 + \eta_1\dot{\gamma}e^{t_1\dot{\gamma}}$ where t_1 is a time constant with the unit of seconds. Another suggested model called the CCJ model (eq. 2) with 6 parameters is known to fit various ER fluids well especially at a low shear rate regime as following:

$$\tau = \frac{\tau_0}{1+(t_1\dot{\gamma})^{\alpha}} + \eta_{\infty}\left[1+\frac{1}{(t_2\dot{\gamma})^{\beta}}\right]\dot{\gamma} . \tag{2}$$

Here, τ_0 is the yield stress, η_{∞}. is the viscosity at a high shear rate. The exponent α and β are related to the decrease and increase in the shear stress, β has the range $0 < \beta \leq 1$, since $d\tau/d\dot{\gamma} \geq 0$. The parameters t_1 and t_2 are time constants. The optimal fitting parameters used for these three models are summarized in Table 1. It is obvious that the CCJ model can cover the curves better especially at low shear rates and higher electric fields, compared with both Bingham and De Kee-Turcotte models.

On the other hand, to incorporate both the stress changes of structural realignment at low shear rates and the yielding

Table 1. The optimal parameters appeared in each model equation obtained from the flow curves of 15 wt% PS/GO based ER fluid (Reprinted from Zhang, *et al*., 2011).

Model	Parameters	Electric field strength (kV/mm)			
		1.0	2.0	3.0	4.0
Bingham	τ_0	4.8	12	40	72
	η_0	0.16	0.13	0.08	0.08
De Kee-Turcotte	τ_0	5	12	36	65
	η_1	0.12	0.1	0.13	0.1
	t_1	0.0003	0.0003	0.0004	0.00001
CCJ	τ_0	6.9	10.8	77	120
	t_1	0.005	0.0008	0.45	0.1
	α	0.1	0.38	0.16	0.32
	η_∞	0.18	0.18	0.15	0.22
	t_2	0.17	0.068	0.76	0.02
	β	0.79	0.99	0.69	0.90

behavior at high shear rates, Seo *et al*. (2011) proposed a following four-parameter model

$$\tau = \tau_y\left(1-\frac{(1-\exp(-a\dot{\gamma}))}{(1+(a\dot{\gamma})^{\alpha})}\right)+\eta\dot{\gamma} \tag{3}$$

where τ_y is the yield shear stress, h is the shear viscosity, and a is the time constant, *i.e.*, the reciprocal of critical shear rate for aligned particle structure deformation (Seo and Seo, 2012). A power-law form was used for the shear rate dependence in the first term denominator to account for the breakup and reformation of the aligned particle structure; this form is similar to the von-Mises criterion for the constitutive relation of stress-strain behavior (Papanastasiou, 1987).

The dynamic yield stress for 10 vol% PANI /GO composite based ER fluid was plotted as a function of the electric field strength in log-log scale curves. In general, the dependency of the dynamic yield stress with the electric field strength was presented by a power law relationship as follows:

$$\tau_y \propto E^m \tag{4}$$

where m=2.0 is suggested by the polarization model, and m=1.5 is suggested for the conduction model (Klingerberg *et al*., 1991). The ER response was affected by complicated factors, like a conductivity mismatch, electrical breakdown, interaction between particles and medium. The only power index m appears deficiently. To correlate the dynamic yield

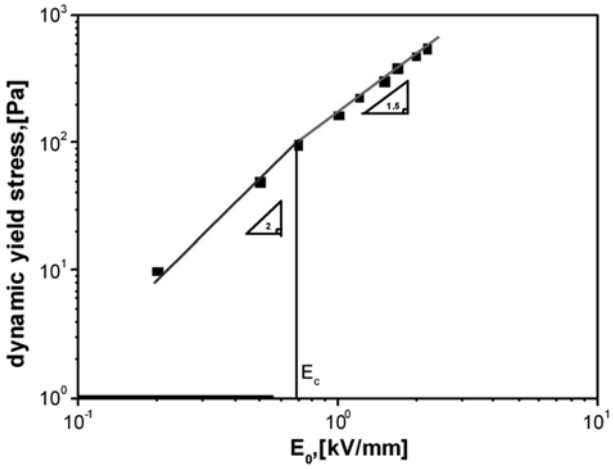

Fig. 4. The dynamic yield stress versus electric field strength for 10 vol% PANI/GO composite dispersed in silicone oil (Reprined from Zhang *et al*., 2012a).

stress for a broad range of electric field strengths, Choi *et al*., 2001 introduced a simple hybrid universal yield stress equation (Eq. (5)) with the parameter named critical electric field E_c, which can be obtained by the crossover point of the slopes corresponding to the polarization model and conductivity model among all ranges of electric field strengths

$$\tau_y(E_0) = \alpha E_0^2\left(\frac{\tanh\sqrt{E_0/E_c}}{\sqrt{E_0/E_c}}\right). \tag{5}$$

Here, the parameter α depends on the dielectric properties of the fluid, particle volume fraction and E_c.

The dynamic yield stress as a function of the electric field strengths was presented in Fig. 3. The estimated E_c was 0.7kV/mm. A single universal curve in Eq. (5) with E_c and $\tau_y(E_c)$ is normalized to collapse the data as given in Eq. (6):

$$\hat{\tau} = 1.313\hat{E}^{3/2}\tanh\sqrt{\hat{E}}. \tag{6}$$

Here, $\hat{E} \equiv E_0/E_c$ and $\hat{\tau} \equiv \tau_y(E_0)/\tau_y(E_c)$. The data obtained from Fig. 3 collapsed onto to a single curve using the normalized universal yield stress Eq. (6) as shown in Fig. 5.

On the other hand, Seo (2011) recently proposed a new simple scaling equation for yield stress based on physical reasoning and the rheological behavior of Bingham fluids. Using a single parameter, he found that the model results correlate well with both ac and dc field data due to the normalization of the data to collapse them onto a single curve.

The flow curves of the pure CI and MWNT/PS/CI particles based MR fluids were characterized at magnetic field strengths ranging from 0 to 343 kA/m with shear rate varied from 0.01 to 500 s^{-1} on a log scale as the high shear rates can result in sample expulsion from the space

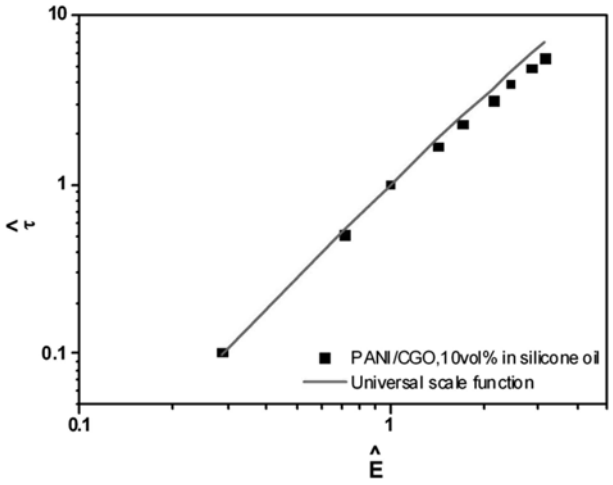

Fig. 5. $\hat{\tau}$ versus $\hat{\dot{E}}$ for GO/PANI composite particles (10 vol.% particle concentration) based ER fluid (Reprined from Zhang *et al*., 2012a).

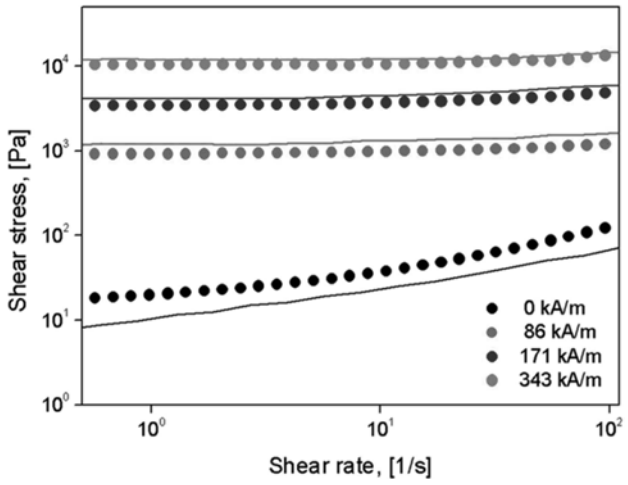

Fig. 6. Rheogram obtained via controlled shear rate mode for 20 vol% of MWNT/PS/CI suspension (points) and pure CI suspension (lines) under different magnetic field strengths (Reprinted from Fang *et al*., 2010a).

between the parallel disks shown in Fig. 6. In the applied external magnetic field, the Bingham fluid behavior was found to characterize the field dependent flow behavior of the MR fluid. Both MR fluids showed a dramatic increase in shear stress along with increasing magnetic field strength. Steady shear stresses, which were identified by showing plateau behavior over the entire shear rate range, were also observed due to the stable field induced chain structures of the dispersed particulates. In contrast with the pure CI suspension, the MWNT/PS/CI suspension displayed a nonzero yield stress at low shear rates which could be explained that the two-step CI microsphere coating process produced a rough particle surface increasing the friction among particles relative to the pure CI particles. Under an applied magnetic field, the rheological properties of the systems displayed a similar dependence on the magnetic field strength and a wide plateau over the shear rates. Unlike the behavior obtained in the absence of a magnetic field, the MWNT/PS/CI suspension yielded a lower shear stress than that of a pure CI suspension under the same magnetic field strength. However, we can easily find that the yield stresses from MR fluids are much higher than those from ER fluids. In addition, compared to the flow curves of ER fluids, MR fluids follow Bingham fluid behaviors (Cheng *et al*., 2009).

It can be also noted that in contrast with the pure CI suspension, another dual-coated system of MWNT/PANI/CI suspension displayed a nonzero yield stress at low shear rates which could be explained that the two-step CI microsphere coating process produced a rough particle surface increasing the friction among particles relative to the pure CI particles (Fang *et al*., 2011). Under an applied magnetic field, the rheological properties of the systems displayed a similar dependence on the magnetic field strength and a wide plateau over the shear rates. Unlike the behavior obtained in the absence of a magnetic field, the MWNT/PANI/CI suspension yielded a lower shear stress than that of a pure CI suspension under the same magnetic field strength (Fang *et al*., 2011).

4. Dispersion Characteristics

Sedimentation ratio is a common criterion of the dispersion stability of a MR fluid. As the particles in the suspension settle, phase boundary between the concentrated turbid suspension and supernatant liquid was observed. The sedimentation profile was defined as the volume fraction of the supernatant liquid in the total fluid and could be calculated from the equation below.

$$\text{Sedimentation ratio} = h/H \times 100\% \quad (7)$$

in which h and H are the height of the supernatant liquid and the height of the entire suspension, respectively.

Fig. 7 shows the sedimentation profile of the MR fluid containing dual-coated carbonyl iron particles by polystyrene and multi-walled carbon nanotube (MWNT/PS/CI) comparing to that of the once-coated PS/CI particles and pure CI particles. As a function of time, MWNT/PS/CI particles indicate the slowest sedimentation velocity during the initial 5 h and then tend to get stable. It is the result of the lower density of the coated particles, which is also one the main reason why coating technology was so attractive in synthesizing MR particles (Liu *et al*., 2012). In addition, the hairy surface of the coated particles by MWNT also delayed the settling of the particles. Therefore, as a conclusion, the MWNT-coated PS/CI particles undergo the slowest sedimentation over 20 h,

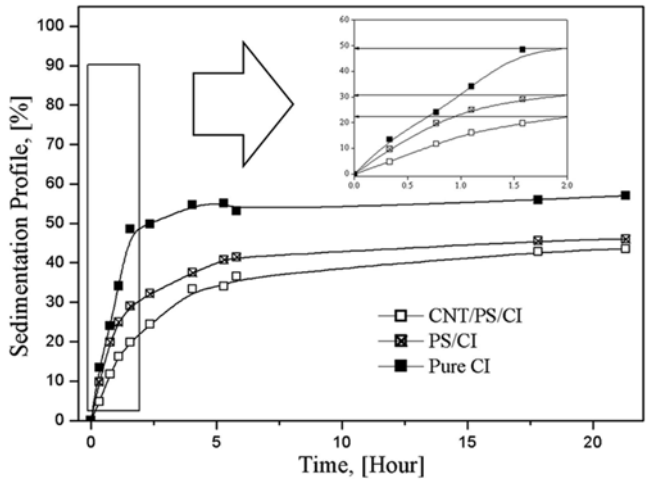

Fig. 7. Sedimentation profile recorded as a function of time for pure CI, PS/CI and MWNT/PS/CI suspensions. The inset figure is a magnified view of sedimentation ratio tested at initial 2 hours (Reprinted from Fang *et al*., 2010a).

consequently meaning that the dual-coated particles exhibit better dispersion stability.

5. Conclusions

In this short review, core–shell structured PS/GO composite synthesized through the strong π–π stacking interaction between PS microspheres and GO sheets was introduced. The ER characteristics of PS/GO composites based ER fluid shows that the CCJ model can fit the flow curves well. At the same time, the MWNT/PS/CI composite was prepared by wrapping the CI particles in a PS shell and a nest via facile dispersion polymerization followed by solvent casting. The coated CI particles displayed slightly lower MR performances under an applied magnetic field because of the weaker saturation magnetization, but enhanced shear behavior due to the rough surface. This novel core-shell structure with a low density and a rough surface improves the sedimentation properties in MR fluid applications.

Acknowledgments

This work was supported by National Research Foundation, Korea (No. 2011-0006592).

References

Barnard, A. S. and I. K. Snook, 2010, Size- and shape-dependence of the graphene to graphane transformation in the absence of hydrogen, *J. Mater. Chem.* **20**, 10459.

Bica, I., 2011, Magnetoresistor sensor with magnetorheological elastomers, *J. Ind. Eng. Chem.* **17**, 83.

Cai, D. and M. Song, 2010, Recent advance in functionalized graphene/polymer nanocomposites, *J. Mater. Chem.* **20**, 7906.

Cheng, H. B., J. M. Wang, Q. J. Zhang, and N. M. Wereley, 2009, Preparation of composite magnetic particles and aqueous magnetorheological fluids, *Smart Mater. Struct.* **18**, 085009.

Cheng, Q., V. Pavlinek, Y. He, C. Li, and P. Saha, 2009, Electrorheological characteristics of polyaniline/titanate composite nanotube suspensions, *Colloid Polym. Sci.* **287**, 435.

Cho, M. S., Y. H. Cho, H. J. Choi, and M. S. Jhon, 2003, Synthesis and electrorheological characteristics of polyaniline-coated poly(methyl methacrylate) microsphere: Size effect, *Langmuir* **19**, 5875.

Cho M. S., H. J. Choi, and M. S. Jhon, 2005, Shear stress analysis of a semiconducting polymer based electrorheological fluid system, *Polymer* **46**, 11484.

Choi H. J., M. S. Cho, J. W. Kim, C. A. Kim, and M. S. Jhon, 2001, A yield stress scaling function for electrorheological fluids, *Appl. Phys. Lett.* **78**, 3806.

Choi, H. J. and M. S. Jhon, 2009, Electrorheology of polymers and nanocomposites, *Soft Matter* **5**, 1562.

Fang, F. F., H. J. Choi, and Y. Seo, 2010a, Sequential coating of magnetic carbonyliron particles with polystyrene and multi-walled carbon nanotubes and its effect on their magnetorheology. *ACS Appl. Mater. Inter.* **2**, 54.

Fang, F. F., Y. D. Liu, H. J. Choi, and Y. Seo, 2011, Core-shell structured carbonyl iron microspheres prepared via dual-step functionality coatings and their magnetorheological response. *ACS Appl. Mater. Inter.* **3**, 3487.

Fang, M., L. Long, W. Zhao, L. Wang, and G. Chen, 2010b, pH-responsive chitosan-mediated graphene dispersions, *Langmuir* **26**, 16771.

Hiamtup, P., A. Sirivat, and A. M. Jamieson, 2010, Strain-hardening in the oscillatory shear deformation of a dedoped polyaniline electrorheological fluid, *J. Mater. Sci.* **45**, 1972.

Hong, J. Y. and J. Jang, 2012, Highly stable, concentrated dispersions of graphene oxide sheets and their electro-responsive characteristics, *Soft Matter* **8**, 3348.

Hummers, W. S. and R. E. Offeman, 1958, Preparation of graphitic oxide, *J. Am. Chem. Soc.* **80**, 1339.

Huo, L., J. R. Li, and F. H. Liao, 2011, The comparison between carboxyl, amido and hydroxyl group in influencing electrorheological performance. *Korea-Aust. Rheol. J.* **23**, 17.

Jang, I. B., H. B. Kim, J. Y. Lee, J. L. You, H. J. Choi, and M. S. Jhon, 2005, Role of organic coating on carbonyl iron suspended particles in magnetorheological fluids, *J. Appl. Phys.* **97**, 10Q912.

Kampouris, D. K. and C. E. Banks, 2010, Exploring the physicoelectrochemical properties of graphene, *Chem. Comm.*, **46**, 8986.

Kim, Y. D. and J. C. Jung, 2010, Effect of aliphatic spacer length on the electrorheological properties of side-chain liquid crystalline polymer-silica composite suspensions, *Macromol. Research* **18**, 1203.

Klingerberg, D. J., F. van Swol, and C. F. Zukoski, 1991, The small shear rate response of electrorheological suspensions. II. Extension beyond the point–dipole limit, *J. Chem. Phys.* **94**, 6170.

Kee, D. D. and G. Turcotte, 1980, Viscosity of biomaterials, *Chem. Eng. Comm.* **6**, 273.

Lee, I. S., M. S. Cho, and H. J. Choi, 2005, Preparation of polyaniline coated poly(methyl methacrylate) microsphere by graft polymerization and its electrorheology. *Polymer* **46**, 1317.

Li, W. H. and X. Z. Zhang, 2008, The effect of friction on magnetorheological fluids, *Korea-Aust. Rheol. J.* **20**, 45.

Lim, S. T., H. J. Choi, and M. S. Jhon, 2005, Magnetorheological characterization of carbonyl iron-organoclay suspensions, *IEEE Trans. Magn.* **41**, 3745.

Liu, Y. D., F. F. Fang, and H. J. Choi, 2010, Core-shell structured semiconducting PMMA/polyaniline snowman-like anisotropic microparticles and their electrorheology, *Langmuir* **26**, 12849.

Liu, Y.D., H.J. Choi, and S.B. Choi, 2012, Controllable fabrication of silica encapsulated soft magnetic microspheres with enhanced oxidation-resistance and their rheology under magnetic field, *Colloid Surf. A- Physicochem. Eng. Asp.* **403**, 133.

Ngatu, G.T. and N.M. Wereley, 2007, Viscometric and sedimentation characterization of bidisperse magnetorheological fluids, *IEEE Trans. Magn.* **43**, 2474.

Niu, X., M. Zhang, J. Wu, W. Wen, and P. Sheng, 2009, Generation and manipulation of "smart" droplets, *Soft Matter* **5**, 576.

Orihara, H., Y. Nishimoto, K. Aida, and Y. H. Na, 2011, Three-dimensional observation of an immiscible polymer blend subjected to a step electric field under shear flow, *Phys. Rev. E* **83**, 026302.

Papanastasiou, T. C., 1987, Flows of materials with yield, *J. Rheol.* **31**, 385.

Sedlacik, M., V. Pavlinek, P. Saha, P. Svrcinova, P. Filip, and J. Stejskal, 2010, Rheological properties of magnetorheological suspensions based on core–shell structured polyaniline-coated carbonyl iron particles, *Smart Mater. Struct.* **19**, 115008.

Seo, Y., 2011, A new yield stress scaling function for electrorheological fluids, *J. Non-Newtonian Fluid Mech.* **166**, 241.

Seo, Y. P., H. J. Choi, and Y. Seo, 2011, Analysis of the flow behavior of electrorheological fluids with the aligned structure reformation, *Polymer* **52**, 5695.

Seo, Y. P. and Y. Seo, 2012, Modeling and analysis of electrorheological suspensions in shear flow, *Langmuir* **28**, 3077.

Stankovich, S., D. A. Dikin, R. D. Piner, K. A. Kohlhaas, A. Kleinhammes, Y. Jia, Y. Wu, S. T. Nguyen, and R. S. Ruoff, 2007, Synthesis of graphene-based nanosheets via chemical reduction of exfoliated graphite oxide, *Carbon* **45**, 1558.

Tang, X., X. Zhang, R. Tao, and Y. Rong, 2000, Structure-enhanced yield stress of magnetorheological fluids, *J. Appl. Phys.* **87**, 2634.

Tian, Y., Y. Meng, and S. Wen, 2001, Electrorheology of a zeolite/silicone oil suspension under dc fields, *J. Appl. Phys.* **90**, 493.

Tian, Y., J. Jiang, Y. Meng, and S. Wen, 2010, A shear thickening phenomenon in magnetic field controlled-dipolar suspensions, *Appl. Phys. Lett.* **97**, 151904.

Wang, B., M. Zhou, Z. Rozynek, and J. O. Fossum, 2009, Electrorheological properties of organically modified nanolayered laponite: influence of intercalation, adsorption and wettability, *J. Mater. Chem.* **19**, 1816.

Wu, Y. H., T. Yu, and Z. X. Shen, 2010, Two-dimensional carbon nanostructures: Fundamental properties, synthesis, characterization, and potential applications, *J. Appl. Phys.* **108**, 071301.

Yi, H., H. Song, and X. Chen, 2007, Carbon nanotube capsules self-assembled by W/O emulsion technique, *Langmuir* **23**, 3199.

Yin, J., X. Zhao, L. Xiang, X. Xia, and Z. Zhang, 2009, Enhanced electrorheology of suspensions containing sea-urchin-like hierarchical Cr-doped titania particles, *Soft Matter* **5**, 4687.

Yin, J., X. Xia, X. Wang, and X. Zhao, 2011, The electrorheological effect and dielectric properties of suspensions containing polyaniline@titania nanocable-like particles, *Soft Matter* **7**, 10978.

Zhang, X., W. Li, and X. L. Gong, 2008, Study on magnetorheological shear thickening fluid, *Smart Mater. Struct.* **17**, 015051.

Zhang, W. L., B. J. Park, and H. J. Choi, 2010, Colloidal graphene oxide/polyaniline nanocomposite and its electrorheology. *Chem. Comm.* **46**, 5596.

Zhang, W. L., Y. D. Liu, and H. J. Choi, 2011, Graphene oxide coated core-shell structured polystyrene microspheres and their electrorheological characteristics under applied electric field. *J. Mater. Chem.* **21**, 6916.

Zhang, W. L., Y. D. Liu, and H. J. Choi, 2012a, Fabrication of semiconducting graphene oxide/polyaniline composite particles and their electrorheological response under an applied electric field, *Carbon* **50**, 290.

Zhang, W. L., Y. D. Liu, H. J. Choi, and S. G. Kim, 2012b, Electrorheology of graphene oxide, *ACS Appl. Mater. Inter.* **4**, 2267.